

Modeling the electronic behavior of  $\text{-LiV}_2\text{O}_5$ : a microscopic study.Roser Valent<sup>1</sup>, T. Saha-Dasgupta<sup>2</sup>, J.V. Alvarez<sup>1</sup>, K. Pozgajic<sup>1</sup> and Claudius Gros<sup>1</sup><sup>1</sup>Fakultät 7, Theoretische Physik, University of the Saarland, 66041 Saarbrücken, Germany.<sup>2</sup>Bose National Centre for Basic Sciences, JD Block, Sector 3, Salt Lake City, Kolkata 700098, India.

(January 31, 2020)

We determine the electronic structure of  $\text{-LiV}_2\text{O}_5$ , which has two inequivalent vanadium ions, V(1) and V(2), via density-functional calculations. We find a relative V(1)-V(2) charge ordering of roughly 70 : 30. We discuss the possible scenarios compatible with the experimentally observed magnetic behavior, which is that of a one-dimensional spin-1/2 Heisenberg antiferromagnet and give estimates of the basic hopping matrix elements. Comparison with the most studied  $^0\text{-NaV}_2\text{O}_5$  is presented.

PACS numbers: 75.30.Gw, 75.10.Jm, 78.30.-j

Low-dimensional transition metal compounds have been intensively studied in the past years. Among those, a highly discussed material has been  $^0\text{-NaV}_2\text{O}_5$ .

$^0\text{-NaV}_2\text{O}_5$  is believed to be a quarter-filled ladder compound<sup>1,2</sup> with only one equivalent  $\text{V}^{4.5+}$ -site which undergoes a phase transition at  $T_c = 34\text{K}$  where charge ordering<sup>3</sup> occurs ( $2\text{V}^{4.5+} \rightarrow \text{V}^{4+} + \text{V}^{5+}$ ) simultaneously with the opening of a spin-gap<sup>4</sup>. The nature of this transition is still under discussion<sup>5,6,7</sup>.

A much less studied, though not less interesting system belonging to the same vanadium oxide family is  $\text{-LiV}_2\text{O}_5$ . Susceptibility measurements<sup>8</sup> as well as NMR experiments<sup>9</sup> on this compound suggest a one-dimensional spin-1/2 Heisenberg-like behavior and there is no indication of a phase transition at lower temperatures. To our knowledge, there is no microscopic study on the electronic structure of this material discussing the magnetic interactions responsible for such behavior. We present here a density-functional analysis (DFT) of this system and calculate the possible exchange matrix elements via the Linear Muffin-Tin Orbital (LMTO) based downfolding method<sup>10</sup> and a tight-binding model. We discuss three possible scenarios compatible with the experimental susceptibility for  $\text{-LiV}_2\text{O}_5$ :

- (i) A zig-zag chain model of V(1)-ions.
- (ii) A double-chain model of V(1)-ions.
- (iii) An asymmetric quarter-filled ladder model.

**Crystal structure.**—  $\text{-LiV}_2\text{O}_5$  has a layered structure of  $\text{VO}_5$  square pyramids with lithium ions between the layers. It crystallizes<sup>11</sup> in the orthorhombic centrosymmetric space group  $D_{2h}^{16}$  Pnm and has two crystallographic inequivalent vanadium sites, V(1) and V(2), which form two different zig-zag chains running along the y axis. Within the layers, V(1) $\text{O}_5$  zig-zag chains are

linked to V(2) $\text{O}_5$  zig-zag chains by corner sharing via the bridging O(1). The existence of two types of V-sites has been also verified by NMR experiments<sup>13</sup>.

In Fig. 1 one of the two equivalent xy-planes of  $\text{-LiV}_2\text{O}_5$  is shown in a xz-cut in comparison with the corresponding xy-planes of  $^0\text{-NaV}_2\text{O}_5$ . The angle between the basal plane of the (nearly) square V(1) $\text{O}_5$ /V(2) $\text{O}_5$  pyramids and the x-axis is about  $+30^\circ / -30^\circ$  respectively for  $\text{-LiV}_2\text{O}_5$ . The basal plane of the  $\text{VO}_5$  pyramids in  $^0\text{-NaV}_2\text{O}_5$  is, on the other hand, nearly parallel to the x-axis. Note that the  $\text{VO}_5$  square pyramids are oriented along x as down-down-up-up in  $^0\text{-NaV}_2\text{O}_5$  while in  $\text{-LiV}_2\text{O}_5$  the orientation is down-up-down-up.

From the structural analysis it has been proposed<sup>11</sup> that the oxidations of V(1) and V(2) are, respectively,  $\text{V}^{4+}$  and  $\text{V}^{5+}$ . The temperature dependence of the susceptibility ( $\chi$ ) follows that of a one-dimensional spin-1/2 Heisenberg model with an exchange interaction of  $J_{\text{exp}} = 308\text{K}$  and a gyromagnetic factor  $g = 1.8$ . Note that depending on the magnitude of the exchange couplings,  $J_1$  between V(1)-ions in edge-shared pyramids and  $J_b$  between V(1)-ions in corner-shared pyramids along y the system can be treated as Heisenberg zig-zag chains ( $J_1 = J_b$ ) or as Heisenberg double-linear chains ( $J_1 \neq J_b$ ), compare with Fig. 2.

A third possible interpretation of the nature of  $\text{-LiV}_2\text{O}_5$  compatible with the experimental susceptibility relies on the possibility of a partially charge-ordered system i.e. V(1)-sites somewhat closer to  $\text{V}^{4+}$ -oxidation and V(2)-sites closer to  $\text{V}^{5+}$ -oxidation. A picture of an asymmetric ladder with one electron per V(1)-O-V(2) rung would then describe the system in analogy to  $^0\text{-NaV}_2\text{O}_5$  where the magnetic interactions among the constituent ladders are weak<sup>12</sup>. In the following, we will investigate these three scenarios.

**Band structure.**— We have calculated the energy bands (see Fig. 3) of  $\text{-LiV}_2\text{O}_5$  within DFT by employing the full-potential linearized augmented plane wave code WIEN97<sup>14</sup> and by LMTO<sup>15</sup> based on the Stuttgart TB LMTO-47 code. We find complete agreement in between these two calculations.

The overall band picture for  $\text{-LiV}_2\text{O}_5$  (Fig. 3) is similar to that of  $^0\text{-NaV}_2\text{O}_5$ <sup>1</sup>. The V-3d states give the predominant contribution to the bands at the Fermi level and up to 4eV above it. The lower valence bands are mainly O-2p states and are separated by a gap of 2.2eV from the bottom of the V-3d bands. There is a nonequivalent contribution from the two types of V-sites, V(1) and V(2). The four lowest-lying 3d bands

at the Fermi level are half-filled<sup>16</sup> and are made up predominantly of V (1)-3d and of V (2)-3d states in the ratio  $p(1)=p(2) = 2:1$  and  $3:1$  depending on the  $k$ -values. The next four bands less than 1 eV above the Fermi level also exhibit a mixture of V (1)-3d and V (2)-3d character.

The vanadium bands at the Fermi level are of  $d_{xy}$  symmetry (global symmetry) with a certain admixture with the  $d_{yz}$  state due to the rotation of the basal plane of the V (1/2)O<sub>5</sub> pyramids with respect to the  $x$ -axis (see Fig. 1). The degree of admixture for both vanadium types is such that the respective V-3d orbitals point—as in <sup>0</sup>-NaV<sub>2</sub>O<sub>5</sub><sup>1</sup>—roughly towards the bridging oxygens. In this sense, one can regard the electronic active V (1)-3d and V (2)-3d orbitals as  $d_{xy}$  orbitals rotated around the  $y$ -axis by angles  $\phi_1 = 35^\circ$  and  $\phi_2 = 28^\circ$  respectively (see Fig. 4).

The most notable difference between the band-structure of <sup>-</sup>LiV<sub>2</sub>O<sub>5</sub> and <sup>0</sup>-NaV<sub>2</sub>O<sub>5</sub> is the band-splitting at the X and T points in <sup>-</sup>LiV<sub>2</sub>O<sub>5</sub>, which is absent in <sup>0</sup>-NaV<sub>2</sub>O<sub>5</sub>. This splitting is due to the existence of two different V-sites in <sup>-</sup>LiV<sub>2</sub>O<sub>5</sub> as we will see in the next paragraph. The fact that this splitting is big, close to the overall bandwidth, indicates already that the microscopic parameters associated with the V (1) and V (2) sites must differ substantially.

Also note that the splitting of the bands at the Fermi level due to the existence of two  $xy$ -planes in the crystallographic unit-cell of <sup>-</sup>LiV<sub>2</sub>O<sub>5</sub> is small and does not occur along the path Z-U-R-T-Z. We will concentrate upon the discussion of the in-plane dispersion in what follows.

Microscopic parameters.— In order to determine the microscopic model appropriate for <sup>-</sup>LiV<sub>2</sub>O<sub>5</sub> we have analyzed the band-structure shown in Fig. 3 by a (minimal) tight-binding model with one orbital per vanadium site, see Fig. 2, which generalizes the tight-binding model appropriate for <sup>0</sup>-NaV<sub>2</sub>O<sub>5</sub> to the case of two different V-sites. A straightforward fit, e.g. by least-squares, is not possible since the lower unoccupied V-bands (roughly in between 0.5–1.0 eV), are strongly hybridized with the O- $p$  orbitals and in order to describe the low-energy physics of this system these bands should also be considered. In recent years<sup>10</sup>, a new version of the LMTO method has been proposed and implemented which is proved to be powerful in providing an effective orbital representation of the system by integrating out the higher degrees of freedom using the so-called downfolding technique. The usefulness of the method lies in taking into account proper renormalization effects. However, the Fourier transform of the downfolded Hamiltonian to extract the tight-binding parameters, results in long-ranged hopping matrix elements.

We have therefore considered a combination of both methods. We use only the short-ranged hopping matrix elements (see Fig. 2) provided by the downfolding procedure as an input for the tight-binding model. These matrix elements are then optimized to reproduce the behavior of the ab-initio bands near the Fermi level. The result and the parameters (apart from an overall constant

energy) of the optimal fit are shown in Fig. 5.

From the relative weight between the V (1) and the V (2) contributions near the Fermi level,  $p(1)=p(2)$ , we learn that there must be a substantial on-site energy  $e_0$  for the V (1=2) orbitals respectively. We find  $e_0 = 0.15$  eV. The rung-hopping matrix element  $t_a$  may be expected, on the other hand, to be quite close to the one obtained for <sup>0</sup>-NaV<sub>2</sub>O<sub>5</sub><sup>20</sup> since the large bending angle V (1)-O (1)-V (2) should not substantially affect the  $\sigma$ -bonding via the O (1)- $p_y$  orbital. Indeed, we find  $t_a = 0.35$  eV. We can check whether our estimates for  $e_0$  and  $t_a$  lead to the correct V (1)-V (2) charge ordering. By diagonalizing a simple two-site rung model we find the relation

$$\frac{e_0}{t_a} = \frac{p(2) - p(1)}{2 \cdot p(1)p(2)}; \quad (1)$$

which yields  $p(1)=p(2) = 2:3$  for  $e_0=t_a = 0.15=0.35$ , i.e.  $p(1) = 0.7$  and  $p(2) = 0.3$ , in agreement with the DFT results.

We note next, that the crossing along  $-Y$  and Z-U respectively can be described (within a V-model) only by a considerable  $t_2^{(1=2)}$ , as it has been noted previously<sup>1</sup>. Recently Yaresko et al.<sup>17</sup> have discussed that this matrix element arises naturally when one integrates out the coupling between two leg-oxygens of two adjacent edge-sharing VO<sub>5</sub> pyramids. Our results  $t_2^{(1)} = 0.05$  eV and  $t_2^{(2)} = 0.02$  eV are close to the values obtained for <sup>0</sup>-NaV<sub>2</sub>O<sub>5</sub><sup>20</sup>.

A substantial diagonal hopping matrix element  $t_d$  is needed in order to explain the fact that the dispersion along  $-Y$  of the lower four V-bands has an opposite behavior with respect to the upper four V-bands<sup>18</sup>, as has been pointed out independently for <sup>0</sup>-NaV<sub>2</sub>O<sub>5</sub> by Yaresko et al.<sup>17</sup>. The substantial contribution of  $t_d$  can be explained by effective V-O-O-V exchange paths<sup>17;19</sup>. Our result for <sup>-</sup>LiV<sub>2</sub>O<sub>5</sub>,  $t_d = 0.10$  eV, is slightly larger than the one obtained for <sup>0</sup>-NaV<sub>2</sub>O<sub>5</sub><sup>20</sup>. This is partly due to the fact that the bandwidth of the lower V-d band is with 0.66 eV slightly lower than the 0.7 eV of <sup>0</sup>-NaV<sub>2</sub>O<sub>5</sub>. The hopping matrix element along the V (1) leg,  $t_b^{(1)} = 0.06$  eV has a similar value to the one for <sup>0</sup>-NaV<sub>2</sub>O<sub>5</sub>, though the sign of the effective V (2)-leg hopping parameter,  $t_b^{(2)} = 0.02$  eV, is opposite to the expected one.

The result for  $t_1^{(2)} = 0.05$  eV might have been expected since its corresponding value for <sup>0</sup>-NaV<sub>2</sub>O<sub>5</sub> is small<sup>20</sup>. The result  $t_1^{(1)} = 0.18$  eV is, on the other hand, substantially larger and needs some explanation. In terms of the bandstructure,  $t_1^{(1)}$  is determined predominantly by the large splitting of the V-d bands<sup>21</sup> at X and T (see Figs. 3 and 5). Also, it has been noted previously<sup>1;2</sup> in the context of <sup>0</sup>-NaV<sub>2</sub>O<sub>5</sub> that the bare two-center Slater-Koster matrix elements contributing to  $t_1$  can be as large as 0.3 eV. The effective  $t_1$  is reduced from the bare two-center matrix element by the rotation of

the V-3d orbitals about the crystallographic y-axis and by interference from three-center term  $s^{119}$ . The contribution from V-O-V exchange paths depends strongly on the relative positions of the three atoms. We have performed for  $\text{LiV}_2\text{O}_5$  a Slater-Koster analysis and found that due to interference effects in between the respective dd and dd contributions, the V(2)-V(2) matrix element contributing to  $t_1^{(2)}$  is smaller than the V(1)-V(1) matrix element contributing to  $t_1^{(1)}$ . In addition, the exchange along V(1)-O(4)-V(1) contributing to  $t_1^{(1)}$  was found to be substantially larger than the exchange V(2)-O(5)-V(2) contributing to  $t_1^{(2)}$ . The particular V-O-V distances and angles lead therefore to different  $t_1^{(1)}$  and  $t_1^{(2)}$ .

**Microscopic model.**— The microscopic model corresponding to the results shown in Fig. 5 is that of a spin-1/2 antiferromagnetic Heisenberg chain where the magnetic moments are associated dominantly with the sites of the V(1) ions in  $\text{LiV}_2\text{O}_5$ , the contribution is  $p(1) = 0.7$ . The contribution of about  $p(2) = 0.3$  of the V(2) to the magnetic moment on a V(2)-O(1)-V(1) rung has nevertheless important consequences for the underlying microscopic model. For negligible values of  $p(2)$  the microscopic model could be considered as that of a zig-zag chain with a  $J = 4 t_1^{(1)2} = U$ , since  $t_b^{(1)} = 0.06 \text{ eV}$  is smaller than  $t_1^{(1)} = 0.18 \text{ eV}$ . In the presence of a non-negligible value of  $p(2)$  the effective hopping matrix element  $t_b^{(\text{eff})}$  in between two asymmetric rung states along b is

$$t_b^{(\text{eff})} = p(1)t_b^{(1)} + p(2)t_b^{(2)} = \frac{p}{2} \frac{t_1^{(1)2}}{p(1)p(2)t_d} = 0.127 \text{ eV}$$

Then, using the expression  $J_b = 2 t_b^{(\text{eff})2} = E_c$ , and assuming that the charge-transfer gap is  $E_c = 0.7 \text{ eV}$  as in  $\text{NaV}_2\text{O}_5$ <sup>22</sup> we obtain  $J_b = 540 \text{ K}$  which overestimates somewhat the experimental value  $J_{\text{exp}} = 308 \text{ K}$ .

The relative large value of  $t_1^{(1)} = 0.18 \text{ eV}$  might, at first sight, indicate strong inter-ladder couplings which are not observed experimentally. This can be understood due to the cancelling effect in between different terms contributing to the interchain magnetic exchange  $J_a$  from intermediate singlet and intermediate triplet states<sup>2</sup>.

**Conclusions.**— We have presented an analysis of DFT band-structure calculations for  $\text{LiV}_2\text{O}_5$ . From our results, we conclude that  $\text{LiV}_2\text{O}_5$  could be viewed as a spin-1/2 asymmetric quarter-filled ladder compound. Still, such an interpretation doesn't exclude the possibility of considering the system as double chains with distributed moments since both interpretations are very similar and only differ in the degree of the moment localization. Either of those models would explain the spin wave excitation spectrum obtained by inelastic neutron scattering experiments<sup>23</sup>. Finally, we observe that small distortions in the lattice may have substantial effects on the interladder V-V hopping matrix element  $t_1$ .

**Acknowledgments.**— This work was partially supported

by the DFG. One of us (R.V.) would like to thank C.O. Rodriguez for helpful advice regarding the WIEN 97 code and A.K. Okal for providing the graphics XCrysDen code.

- <sup>1</sup> H. Smolinski, C. Gros, W. Weber, U. Peuchert, G. Roth, M. Widen and C. Geibel, Phys. Rev. Lett. 80, 5164 (1998).
- <sup>2</sup> P. Horsch and F. Mack, Eur. Phys. J. B 5, 367 (1998).
- <sup>3</sup> T. Oham, H. Yasuoka, M. Isobe, and Y. Ueda, Phys. Rev. B 59, 3299 (1999).
- <sup>4</sup> M. Isobe and Y. Ueda, J. Phys. Soc. Jpn. 65, 1178 (1996).
- <sup>5</sup> see for instance J. Ludecke, A. Jobst, S. van Smalen, E. Morre, C. Geibel and H.-G. Krane, Phys. Rev. Lett. 82, 3633 (1999). J. L. de Boer, A. M. Meetsma, J. Baas and T. T. M. Palstra, Phys. Rev. Lett. 84, 3962 (2000).
- <sup>6</sup> C. Gros, R. Valent, J.V. Alvarez, K. Hamacher, and W. Wenzel, Phys. Rev. B 62, R14617 (2000). S. Trebst and A. Sengupta, Phys. Rev. B 62, R14613 (2000). A. Honecker and W. Brenig, Phys. Rev. B (in press).
- <sup>7</sup> A. Bemet, T. Chatterji, P. Thalmeier and P. Fulde, Sissa, cond-mat/0012327.
- <sup>8</sup> M. Isobe and Y. Ueda, J. Phys. Soc. Jpn. 65, 3142 (1996).
- <sup>9</sup> N. Fujiwara, H. Yasuoka, M. Isobe, Y. Ueda, and S. Maegawa, Phys. Rev. B 55, R11945 (1997).
- <sup>10</sup> See O.K. Andersen and T. Saha-Dasgupta, Phys. Rev. B 62, R16219 (2000) and references therein.
- <sup>11</sup> J. Galy and A. Hardy, Acta Cryst. 19, 432 (1955). D.N. Anderson and R.D. Willett, Acta Cryst. B 27, 1476 (1971).
- <sup>12</sup> C. Gros and R. Valent, Phys. Rev. Lett. 82, 976 (1999).
- <sup>13</sup> N. Fujiwara, H. Yasuoka, M. Isobe, and Y. Ueda, Phys. Rev. B 58, 11134 (1998).
- <sup>14</sup> P. Blaha, K. Schwarz and J. Luitz, WIEN 97, A Full Potential Linearized Augmented Plane Wave Package for Calculating Crystal Properties, (Karlheinz Schwarz, Techn. Univ. Wien, Vienna 1999). ISBN 3-9501031-0-4. [Updated version of P. Blaha, K. Schwarz, P. Sorantin, and S.B. Trickey, Comp. Phys. Commun. 59, 399 (1990)].
- <sup>15</sup> O.K. Andersen, Phys. Rev. B 12, 3060 (1975).
- <sup>16</sup> Note that the unit cell of  $\text{LiV}_2\text{O}_5$  corresponds to four formula units.
- <sup>17</sup> A.N. Yaresko, V.N. Antonov, H. Eschrig, P. Thalmeier and P. Fulde, Phys. Rev. B 62, 15538 (2000).
- <sup>18</sup> The dispersion of the antibonding/bonding V-bands in  $\text{NaV}_2\text{O}_5$  is  $t_a + 2(t_b - t_d) \cos(k_y)$ . In order to obtain an opposite dispersion<sup>1;17</sup> one needs  $t_d > t_b$ . The bandwidth  $0.7 \text{ eV} = 4t_b - t_d$  of the bonding orbital and the smaller bandwidth  $0.1 \text{ eV}$  of the antibonding orbital yield then  $t_d = 0.095 \text{ eV}$  and  $t_b = 0.08 \text{ eV}$ .
- <sup>19</sup> H. Smolinski, dissertation, Dortmund 1998.
- <sup>20</sup> The tight-binding parameters for  $\text{NaV}_2\text{O}_5$  are<sup>1;17;18</sup>  $t_a = 0.375 \text{ eV}$ ,  $t_d = 0.095 \text{ eV}$ ,  $t_b = 0.08 \text{ eV}$ ,  $t_2 = 0.055 \text{ eV}$ . We have reanalyzed the DFT band-structure of  $\text{NaV}_2\text{O}_5$  and found that the effective  $t_1$  is very small.
- <sup>21</sup> For general parameters the tight-binding equation cannot be solved analytically but certain limiting cases can be studied. As a illustration, we note that for  $t_1^{(1)} = t_1^{(2)} = t_1$

$t_b^{(2)} = t_b^{(1)}$  and  $t_0^{(2)} = t_0^{(1)}$  the dispersion of the antibonding/bonding bands at X and T in  $\text{-LiV}_2\text{O}_5$  is given by  
 $\epsilon^2 = (\epsilon_0 + (t_b^{(1)} - t_b^{(2)})^2 - 2t_1)^2 + (t_a + 2t_d)^2$ .  
<sup>22</sup> D. Smirnov et al., Phys. Rev. B 57, R11035 (1998).  
<sup>23</sup> Y. Takeo et al. Jour. Phys. Chem. Solids 60, 1145 (1999).

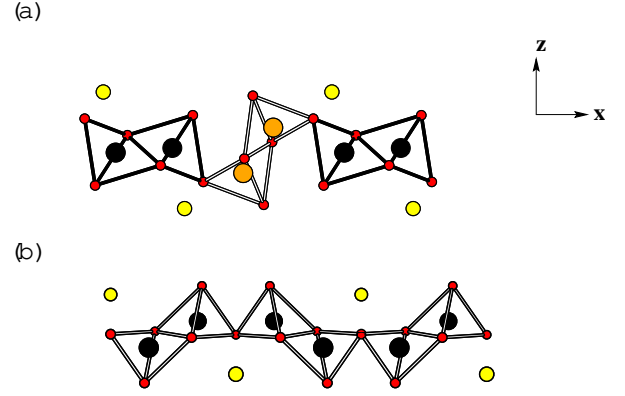


FIG. 1. Crystal structure of (a)  $\text{-LiV}_2\text{O}_5$  and (b)  $^0\text{-NaV}_2\text{O}_5$ . Shown is a (xz) cut through one xy plane. In  $\text{-LiV}_2\text{O}_5$  there are two equivalent xy planes per unit-cell. The large circles are the V-ions, black and grey for V (1) and V (2) respectively in  $\text{-LiV}_2\text{O}_5$ . The oxygens are represented by the smaller circles. In  $\text{-LiV}_2\text{O}_5$  there are two nonequivalent oxygens while in  $^0\text{-NaV}_2\text{O}_5$  there are three. The alkali-ions (Li/Na) are located in between the planes, close to the bridging oxygens.

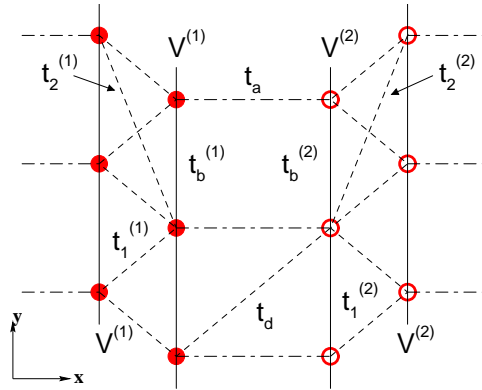


FIG. 2. Hopping parameters used for the tight-binding model for  $\text{-LiV}_2\text{O}_5$ . The arrangement of the V-ions in an xy-plane is topologically identical to the one in  $^0\text{-NaV}_2\text{O}_5$ , i.e. they form a Trelis lattice. The  $t_a$  and the  $t_2^{(1=2)}$  are shown only partially. Not shown are the onsite energies  $\epsilon_0$  of the V (1=2) sites.

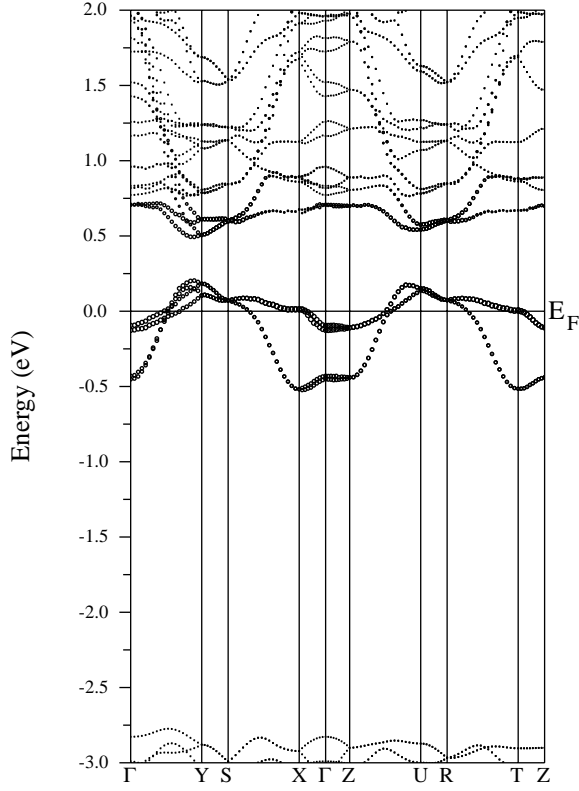


FIG. 3. LDA results for  $\text{LiV}_2\text{O}_5$ . The path is along  $\Gamma = (0,0,0)$ ,  $Y = (0, \pi, 0)$ ,  $S = (\pi, \pi, 0)$ ,  $X = (\pi, 0, 0)$ ,  $\Gamma = (0,0,0)$ ,  $Z = (0,0, \pi)$ ,  $U = (0, \pi, \pi)$ ,  $R = (\pi, \pi, \pi)$ ,  $T = (\pi, 0, \pi)$ ,  $Z = (0,0, \pi)$ . The V(1)- $3d_{xy}$  character of the bands is shown with bigger circles.

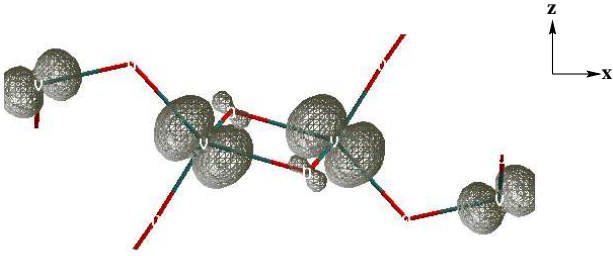


FIG. 4. Electron density of the V-3d bands seen in a (xz) cut. Shown is the isosurface  $0.05 \text{ e}/\text{\AA}^3$ . The bigger lobes correspond to V(1)-3d orbitals and the smaller ones to V(2)-3d orbitals. Note that the tilted orbitals point towards the bridging oxygens (compare with Fig. 1).

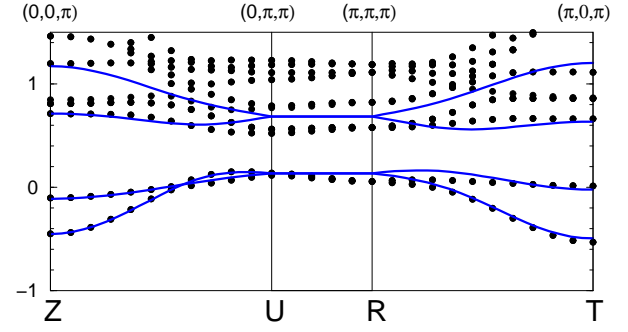


FIG. 5. Comparison of the tight-binding  $t$  (solid lines) with the DFT bands (filled circles). The parameters used (see Fig. 2) are (in eV)  $t_0 = 0.15$ ,  $t_a = 0.35$ ,  $t_d = 0.10$ ,  $t_b^{(1)} = 0.06$ ,  $t_b^{(2)} = 0.02$ ,  $t_1^{(1)} = 0.18$ ,  $t_2^{(1)} = 0.05$ ,  $t_1^{(2)} = 0.05$ ,  $t_2^{(2)} = 0.02$ .